

Incorporating Blood Pressure Load into an Elastomechanical Ventricular Model

MB Mohr¹, RR Schnell¹, G Seemann¹, FB Sachse², O Dössel¹

¹Institute of Biomedical Engineering, Universität Karlsruhe (TH), Germany

²Nora Eccles Harrison Cardiovascular Research and Training Institute, University of Utah, USA

Abstract

Elastomechanical modeling constitutes an essential step for realistic computer simulations of the cardiac system. The deformation of tissue effects e.g. cellular electrophysiology, which is commonly neglected in electrophysiological simulations due to the lack of efficient mechanical models. This work focuses on extending a mechanical deformation model by including blood pressure as endocardial boundary condition. Four phases are distinguished in a normal heart cycle: isovolumic contraction, isotonic contraction, isometric relaxation, and isotonic relaxation. The first three phases were modeled. The methods modeling intraventricular pressure corresponding to contraction phases are illustrated, applied, and discussed. Simulation results show that the mechanical model is capable of incorporating a pressure load leading to a more realistic contraction behavior. Furthermore, the ejection curve resembles in closer detail measured data.

1. Introduction

Computer simulations based on physical models and Virtual Reality techniques have become an appreciated tool for medical doctors and scientists for surgical training and planning. Various mechanical models exist applying e.g. finite element methods and spring mass systems. One part in mechanically modeling the heart consists of acquiring information about anatomy and physiology. The microscopic properties and behavior of myocardial tissue need to be described by mathematical models. The other part consists in modeling blood pressure, valve function, and blood flow.

This work is focused on incorporating blood pressure into an elastomechanical ventricular model [1, 2]. Therefore, the windkessel and wave pressure model from Wang et al. [3] was adapted and the relationship of pressure and intraventricular volume change used.

2. Methods

Two confocal truncated ellipsoids provided the anatomical model of a human left ventricle. In the model, human myocardial fiber orientation was represented by a fiber twist from the inside -75° to the outside 75° surface [2].

A cellular automaton was parameterized by force slopes derived from detailed electrophysiological and force development models. The automaton was used to simulate ventricular excitation propagation and provided a spatial force distribution at $10ms$ time steps during an interval of $1s$. An extended spring-mass system was based on the anatomical model, which applies continuum mechanical methods to model tissue properties e.g. incompressibility of tissue and myocardial stress-strain relationship [2].

2.1. Pressure model

The pressure inside the left ventricular cavity was modeled as a vector field with constant vector orientation but changing vector length during simulation. The vector field was set up by a virtual vertical line coinciding with the main axis of the ellipsoid and ending at a focus point. Vectors were spanned perpendicular from the vertical line to each mass point at the inside surface and furthermore from the focus of the ellipsoid to the masses at the apex (Fig. 1). During simulation the left ventricular pressure was preset

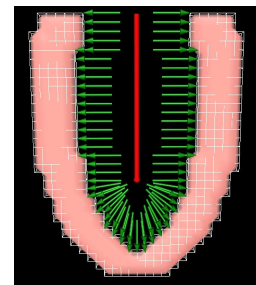


Figure 1. Slice of ventricular model with virtual axis (center) and normalized pressure vectors onto endocardial wall.

and acquired as described below.

2.1.1. Blood pressure

The implementation of blood pressure boundary conditions followed the heart cycle. Four phases are differentiated starting with the systole of the ventricle.

The first phase is called isovolumic contraction. The valves are closed and due to the incompressibility of blood the intraventricular pressure rises at the commencing contraction of myocytes. The ventricle deforms towards a spherical shape.

This phase was modeled by iterative estimation of intraventricular volume and resulting pressure. As the spring mass system does not support isovolumic contraction by default, a contraction was accepted for each simulation step and the changed volume was calculated. The displacements of the masses were reset to the former deformation and a pressure to compensate the volume change was implemented. This procedure was repeated for the first 150ms to simulate isovolumic contraction.

In the second phase the valves open and blood ejects into the aorta. For this phase the isotonic contraction the findings of Wang et al. [3] were applied. They postulated a time domain representation of the ventricular-arterial coupling as a windkessel and wave system. They measured the arterial pressure P_{A0} , the blood ejected into the aorta Q_{in} , the compliance of the aortal tree C , and the effective resistance R of the peripheral systemic circulation. Furthermore, they assumed that the aortal behavior can be expressed as a windkessel, which acts as a hydraulic integrator, where the variation of pressure is directly related to the change in volume and inversely to its compliance. It was possible to calculate the windkessel pressure P_{Wk} . Lighthill et al. [4] proposed, that when considering wave propagation in a reservoir the measured pressure must be the sum of the reservoir pressure and the pressure due to wave motion (excess pressure P_{ex}).

Thus:

$$P_{A0}(t) = P_{Wk}(t) + P_{ex}(t) \quad (1)$$

2.1.2. Windkesselpressure P_{Wk}

In case of Wang et al. [3] the aortic windkessel pressure P_{Wk} depends on the inflow of ejected blood into the aorta Q_{in} , the outflow into the aortal tree Q_{out} and the compliance C of the whole aortal tree.

$$\frac{dP_{Wk}(t)}{dt} = \frac{Q_{in}(t) - Q_{out}(t)}{C} \quad (2)$$

The outflow can be described as a resistive relationship $Q_{out}(t) = \frac{P_{Wk}(t) - P_{\infty}}{R}$ representing the diastolic exponential pressure decay P_{∞} and R the effective resistance of

the peripheral systemic circulation. Substituting $Q_{out}(t)$ into Eq. 2 results in:

$$\frac{dP_{Wk}(t)}{dt} + \frac{P_{Wk}(t) - P_{\infty}}{RC} = \frac{Q_{in}(t)}{C} \quad (3)$$

with a general solution of

$$P_{Wk}(t) - P_{\infty} = (P_0 - P_{\infty})e^{-\frac{t}{RC}} + e^{-\frac{t}{RC}} \int_{t_0}^t \frac{Q_{in}(t')}{C} e^{\frac{t'}{RC}} dt' \quad (4)$$

where t_0 and P_0 are the time and pressure at the onset of ejection.

2.1.3. Pressure due to wave motion P_{ex}

Due to conducted measurements and the application of Lighthills equation (Eq. 1), Wang et al. found that the excess pressure P_{ex} was directly and quite precisely proportional to the aortic inflow Q_{in} . Therefore the proximal resistance R_{prox} was embedded which resembles the characteristic impedance determined by Westerhof et al. [5].

$$P_{ex}(t) = Q_{in}(t)R_{prox} \quad (5)$$

Hence, Eq. 1 can be written as:

$$P_{A0}(t, Q_{in}(t)) = P_{Wk}(t, Q_{in}(t)) + P_{ex}(Q_{in}(t)) \quad (6)$$

Since the pressure of the aorta during ejection resembles that of the ventricle, Eq. 6 can be applied during isotonic contraction phase two. The only changing variables constitute the ejection volume $Q_{in}(t)$, which can be obtained during deformation simulation and time t . The constants can be acquired prior to simulation by measurement or from literature.

Phase three starts with the closing of the valve (t_{cv}) and hence the end of ejection. During this isovolumic relaxation the pressure drops rapidly until it reaches the diastolic atrial pressure (P_{atria}). The pressure characteristic of phase three (P_{P3}) as described in the literature [6] was approximated by an inverse polynomial decay:

$$P_{P3}(t) = \frac{(P_{A0}(t_{cv}) - P_{atria})t_{cv}}{t^8} + P_{atria} \quad (7)$$

During isotonic relaxation the blood refills the ventricle with the aid of the atrial systole until a new ventricular systole commences. The isotonic relaxation describing phase four and the contraction of the atrias were omitted.

One iteration step of the mechanical simulation was set up as follows: The force vector field was loaded onto the fiber springs. Furthermore, the pressure scalars obtained by the methods described above elongated the pressure vectors, which were loaded onto the masses of the endocardial surface. The deformation was evaluated and the resulting intraventricular volume and pressure change calculated.

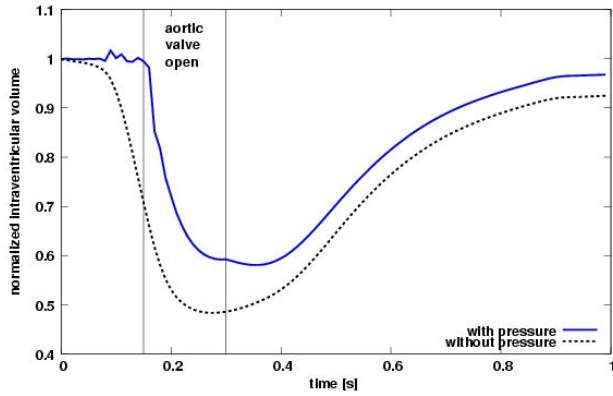


Figure 2. Normalized left intraventricular volume. Slopes describe the decreasing volume during deformation simulation. The opening of the aortic valves are indicated by vertical lines. The slope with applied pressure shows an oscillation of volume due to the regularization of pressure dependent on volume change, a steeper decent during opened valve, and a slight drop after closing of the valve.

3. Results

Deformation simulations were performed with the mechanical model. The mechanical parameter set for the simulations with and without pressure was not varied. The difference of intraventricular volume change in simulations with and without pressure load were recorded (Fig. 2). The volume change in the simulation without pressure shows a smooth curve. The volume decreases from the beginning and rapidly drops between approx. $t = 0.10s$ to $t = 0.13s$. It reaches its minimum at $t = 0.25s$ with a $\Delta V_{max} \approx 0.5$, then gradually rises to approx. 91% of the original volume.

In contrast, the intraventricular volume slope created with pressure load shows a horizontal line with some oscillations until $t = 0.15s$. Furthermore, a steeper decent is visible until $t = 0.3s$ reaching a $\Delta V_{max} \approx 0.4$. Another small decent can be recognized followed by a rise parallel to the slope simulated without pressure to approx. 97% of the volume.

The pressure and the intraventricular volume were recorded during the three phases (Fig. 3). The pressure slope marked by phase one was used to model isovolumic contraction. The curve during phase two was calculated by Eq. 6. The inverse polynomial decay described by Eq. 7 resembles phase three.

The adaption of the model of Wang et al. was implemented for phase two during $t = 0.15s$ and $t = 0.3s$ (Fig. 4), as a change in volume is needed to derive the pressure. The displaced volume Q_{in} was used to calculate P_{ex} , P_{Wk} and P_{A0} . The pressure P_{A0} shows a steep oscillation during the first few milliseconds.

The displacements during simulation were recorded and

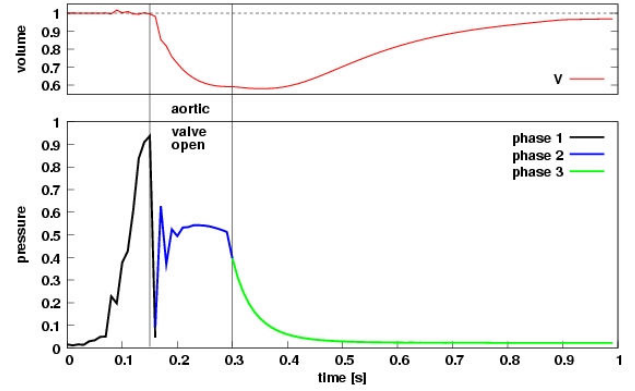


Figure 3. Pressure progression and left intraventricular volume change. The upper graph displays the changing left cavity volume. The lower graph shows the three phases and the according pressure slopes. Vertical lines indicate the opening $t = 0.15s$ and closing $t = 0.3s$ of the aortic valve.

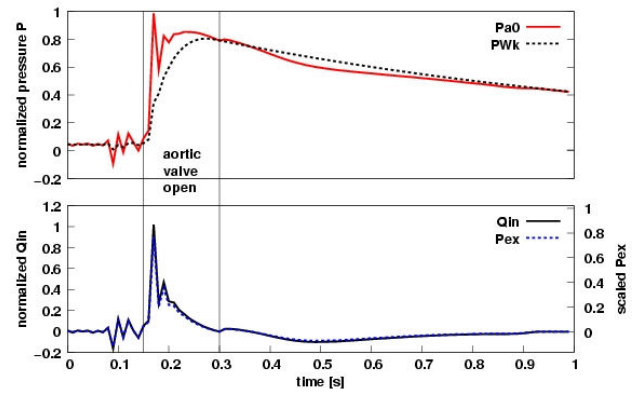


Figure 4. Pressure curves calculated with the model of Wang and Lighthill. Model was applied during open valves only.

displayed for successive timesteps (Fig. 5).

4. Discussion and conclusion

In this work, the intraventricular pressure during a heart cycle was modeled and introduced into a hybrid deformation model for mechanical simulation. The pressure load was implemented by a vector field, which was applied to the intraventricular surface. Furthermore, three out of four phases of the heart cycle were modeled with varying pressure characteristics. Pressure progression, intraventricular volume change, and deformation was recorded and displayed. The pressure characteristics were modeled according to the four heart contraction phases.

Phase one (Fig. 3) shows a steep raise in pressure until $t = 0.15s$, which resembles recordings in the literature [6]. Oscillations in pressure and volume during this

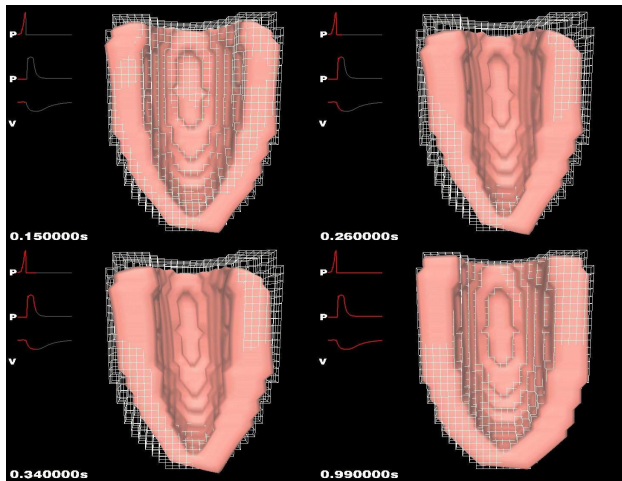


Figure 5. Lateral view of deformed truncated half ellipsoids at successive timesteps. The white wireframe denotes undeformed ellipsoid. The deformation at timestep $0.15s$ shows the isometric contraction phase, whereas at $0.26s$ the ejection phase is presented. The relaxation phase is displayed by the figures at timesteps $0.34s$, and the end of simulation at timestep $0.99s$.

phase are caused by not precise estimate of pressure due to volume change. This can be enhanced by applying smaller timesteps and using mathematical methods to derive adapted pressure values.

During phase two, the findings of Wang et al. were applied. The ejection volume was acquired and resulted in a pressure curve. The oscillations shortly after valve opening are due to the size of timestep, the passover from phase one, and the fast ejection. This phase describes the atrial pressure curve and should start with the offset pressure of the atrial base pressure. Hence, the pressure curve of this phase should commence with an offset given by the peak of phase one. However the forces driving the contraction were not able to sustain the pressure offset given by phase one. The pressure peak of phase one is almost double the size of the pressure generated by the model of Wang et al.. Therefore, further investigations need to be conducted focusing on cross over from pressure phases. Furthermore, the applied forces need to be reevaluated, since electrophysiological and force development models were used based on fully relaxed muscle fibers.

Phase three resembles isovolumic relaxation, where the pressure was modeled by a simple inverse polynomial decay (Eq. 7). However, further evaluation of this function has to be conducted, due to the steep descent. Furthermore, phase four needs to be take into account to complete the model for a full heart cycle.

The normalized intraventricular volume with and without pressure was plotted (Fig. 2). In the isovolumic con-

traction phase the slopes show an explicit difference between simulations with and without pressure. The slope with pressure shows light oscillations between 0 and $0.15s$. The steeper descent in the pressure simulations during opened aortic valve indicates a faster ejection rate. At the border from phase two to three another descent of the volume slope is visible. The investigation showed that the intraventricular pressure in phase three decays faster than the contraction initiating force. Therefore, another light contraction takes place in phase three. However, this issue can be addressed by applying contraction dependent force generation models instead of a static version. Furthermore, the inverse polynomial decay used to model phase three can be reevaluated.

5. Future work

Research will be directed towards applying MRI scans of ventricles to create realistic anatomical models. Furthermore, mathematical models for phases one and three need to be evaluated and applied. The crossover of pressure phases will be enhanced and phase four will be modeled.

References

- [1] Mohr MB, Blümcke LG, Sachse FB, Seemann G, Dössel O. Hybrid deformation model of myocardium. In Proc. CinC, volume 30. 2003; 319–322.
- [2] Mohr MB, Seemann G, Sachse FB, Dössel O. Deformation simulation in an elastomechanical ventricular model. In Proc. CiC. 2004; 777–780.
- [3] Wang JJ, O'Brien AB, Shrive NG, Parker KH, Tyberg JV. Time-domain representation of ventricular-arterial coupling as a windkessel and wave system. *Am J Physiol Heart Circ Physiol* 2003;284(4):H1358–H1368.
- [4] Lighthill J. *Waves in fluids*. Cambridge University Press, 1980; 94–100. ISBN:0-521-21689-3.
- [5] Westerhof N, Sipkema P, van den Bos GC, Elzinga G. Forward and backward waves in the arterial system. *Cardiovasc Res Nov* 1972;6(6):648–656.
- [6] Martini FH. *Fundamentals of Anatomy & Physiology*, volume 5th Edition. Prentice Hall, Inc. Upper Saddle River, NJ, 1998. ISBN 0-13-736265-X.

Address for correspondence:

Matthias B. Mohr
 Institut für Biomedizinische Technik, Universität Karlsruhe (TH)
 Kaiserstr. 12 / 76128 Karlsruhe / Germany
 tel./fax: ++49-721-608-8035/2789
 Matthias.Mohr@ibt.uni-karlsruhe.de